Multi-Area Frequency Restoration Reserve Sizing

Multi-Area Frequency Restoration Reserve Sizing

Panagiotis Pediaditis, *Student Member, IEEE*, Dimitrios Papamatthaiou, Dimitrios Papadaskalopoulos, *Member, IEEE*, Dušan Prešić, Nikos D. Hatziargyriou, *Fellow Member, IEEE*

***Abstract*—Frequency Restoration Reserves are traditionally sized using deterministic methods. The constant growth in non-dispatchable renewable energy, however, is increasing the importance of probabilistic methods for reserve sizing. In addition, as the geographical scope of reserve sizing expands, overall power imbalance stochasticity is reduced. In this paper, we propose a probabilistic method for shared cross-border frequency restoration reserve commitment and sizing, based on the concept of system generation margin and employing mathematical optimization. The aim is to reduce overall reserve volumes and costs. The cross-border interconnection capacities among countries are taken into account, and the shared uncertainty across interconnections is addressed via a novel robust approach. The method is tested on the cross-border system of south-east Europe that includes 9 countries. 5 different operational scenarios are used and a detailed calculation of the uncertainty distributions in each country is employed. Results show that cross-border shared sizing can significantly reduce overall reserve volumes and costs in a secure way.**

***Index Terms*—Balancing area, frequency restoration reserves, multi-area reserve commitment, probabilistic reserves, renewable generation, reserve sizing, reserve commitment, reserve sharing, transmission systems, TSO**

NOMENCLATURE

Indices and Sets

$i, j \in \mathcal{I}$	Balancing areas
$b \in \mathcal{B}$	Interconnections
$n \in \mathcal{N}$	Available FRRs

Parameters

π_n	Cost of FRR n (€/MW)
$\overline{r}_n$	Maximum size of FRR n (MW)
$\underline{F}_b, \overline{F}_b$	Maximum limit of negative and positive power flow on interconnection b (MW)
R_i	Individual FRR requirement of BA i (MW) without cross-border sharing
$\hat{R}_i$	Individual FRR requirement of BA i with cross-border sharing (MW)
$B_{i,n}$	Matrix mapping each FRR n to each BA i
$D^i_{b,j}$	PTDF coupling interconnection b with BA j, with BA i used as the reference
$\hat{D}^i_{b,j}$	PTDF coupling interconnection b with BA j, with BA i used as the reference and factoring only interconnections adjacent to BA i
M_i	System generation margin of BA i without cross-border sharing (r.v.)
M^*_i	System generation margin of BA i with cross-border sharing (r.v.)

Variables

r_n	Committed volume of FRR n (MW)
$\hat{r}_i$	Total FRR volume committed in BA i (MW)
$\tilde{r}_{i,j}$	Shared FRR volume from BA i to BA j (MW)

The work of the authors is partially funded by the H2020 project CROSSBOW–CROSS BOrder management of variable renewable energies and storage units enabling a transnational Wholesale market (Grant No. 773430). This document has been produced with the financial assistance of the European Union.

Panagiotis Pediaditis is with the Department of Electrical and Computer Engineering, Technical University of Athens, Athens, Greece, 15780 (email: panped@mail.ntua.gr)

Dimitrios Papamatthaiou is with the Greek TSO (IPTO), System Operation & Control Department, Athens, Greece, 14568 (email: d.papamatthaiou@admie.gr)

Dimitrios Papadaskalopoulos is with the Department of Electrical and Computer Engineering, University of Patras, Patras, Greece, 26504 (email: dimpap@upatras.gr)

Dušan Prešić is with the Regional Coordination Center (SCC), Development Department, Belgrade, Serbia (email: dusan.presic@scc-rsci.com)

Nikos D. Hatziargyriou is with the Department of Electrical and Computer Engineering, Technical University of Athens, Athens, Greece, 15780, and with the University of Vaasa, Vaasa, Finland, 65200 (email: nh@power.ece.ntua.gr)

I. INTRODUCTION

A. Motivation and Background

The increasing penetration of new energy sources and the digitalisation of the power sector creates new challenges and opportunities for more efficient system operation [1], [2]. In particular, the large-scale integration of renewable generation significantly increases the balancing requirements and costs of power systems [3]. In the European context, reserve products generally include Frequency Containment Reserve (FCR) (primary), Frequency Restoration Reserve (FRR) (secondary) and Replacement Reserve (RR) (tertiary) [4]. FCR is used for keeping frequency deviations at an acceptable range, FRR is responsible for restoring frequency to the nominal value and relieving FCR, and RR is responsible for relieving FRR [5]. FRR is also used to restore the area exchanges to the scheduled values. Before the wide penetration of renewable generation, reserve sizing has been deterministic in nature [6] and calculated on a national basis. However, the large-scale integration of renewable generation in many countries worldwide has highlighted the value of sharing reserves among systems through the available cross-border interconnections, and applying probabilistic principles for their sizing. [7].

Contrary to FCR, which is sized along with the day-ahead (DA) energy scheduling [8], [9], FRR has a longer activation time and can be independently sized in a market different than the DA energy market [4], [10]. This approach is more aligned to the current market structure of most European countries. Namely, DA energy market clearing is performed without consideration of the FRR sizing requirements. The FRR provision is mainly resolved in auctions where large conventional generation units provide reserve blocks with durations that range from a few hours to days [3], [11],

[12]. Such a system provides increased security to the system operator [13].

B. Relevant Literature

The European Union's Third Energy Package [14] requests transmission system operators (TSOs) to facilitate cross-border exploitation of ancillary services [15], including reserves, through regional security coordination centers or other similar mechanisms. Although sharing FRR activation has been taking place in Europe already [13], [16], [17], [18], few works discuss the shared sizing of FRR [19], [20]. For example, commitment and sizing of cross-border FRR resources considering interconnection capacities, has not been sufficiently studied. Furthermore, the Third Energy Package aims at bringing the procurement of balancing services closer to real-time, on the grounds that the required volume and the economic value of such services depend significantly on highly-variable, real-time conditions (especially due to the output of renewable generation). In this context, new EU regulation requires balancing capacity to be procured no more than a DA and for a maximum horizon of one day. In [21], the required DA operating reserve is calculated after load and generation (conventional, wind and solar) schedules are known; in other words, the DA market is closed. Such an approach is important because it is closer to the current market structure in most European countries and is suitable for consideration in the cross-border FRR sizing problem.

In [22], a methodology was proposed by the authors of this paper for sizing FRR among different countries. The method is based on the approach of [21] for FRR sizing in one individual country. The formulation developed in [22] assumed that reserves are sized together for all participating countries. Added uncertainty that comes from sharing is addressed preemptively by updating the imbalance probability distribution in each country.

C. Paper Contributions

This paper proposes a method for the optimal shared sizing of FRR across multiple countries, designed to complement the wholesale energy markets. To the best of our knowledge, [22] and this paper are the first works that propose a method executed after the DA markets are closed and utilises their clearing information. We employ a novel representation of reserve availability while, also, accounting for interconnection capacity limitations. Initially, the individual FRR requirements of each country are calculated probabilistically [21] and, then, the concept of shared uncertainty across interconnections is introduced. Compared to [22], a) a new approach for sharing uncertainty is proposed, b) a more detailed representation of imbalance probability in each country, including consideration for conventional generation, is employed and, c) more extensive case studies are performed.

In summary, the contributions of this paper are the following:

- A method for optimizing cross-border FRR sizing considering uncertainty is presented. This method is applied after the DA market clearing in each country and does not interfere with the existing energy markets.
- An adapted DC power flow representation is used that models *power availability*, which is more suitable for FRR sizing (instead of *power flow*, which is more suitable for reserve activation) and enables satisfaction of cross-border capacity limits.
- Sharing of uncertainty, which is a result of joining individual countries in the FRR sizing process, is considered while each country's FRR requirements are, also, respected.
- The methodology is validated for a wide range of operating conditions using indicative scenarios.

II. Mathematical modelling

A. Model assumptions

The main assumptions are outlined below:

- The proposed method for optimal cross-border FRR sizing is intended to be deployed by a regional coordination entity (such as regional security coordination centers), which, given the amount of FRR required by each national TSO and the submitted reserve bids by reserve providers across the countries of the region, decides on the optimal size of the scheduled reserves and its allocation to the different providers.
- Uncertainties associated with both the national demand of the interconnected countries and their non-dispatchable (wind and solar) and conventional generation are modelled in this paper, as described in detail in subsection II-F.
- Following the approach of [21], [22], the offered price and volume of each reserve bid constitute certain input parameters.
- Similar to [20]–[22] we only focus on procurement of upward reserves.

B. System generation margin

The System Generation Margin (SGM) quantifies the extent to which the generating capacity exceeds the system load, and it constitutes a random variable [21], [23].

Assume one system, Balancing Area (BA) $i \in \mathcal{I}$, where $\mathcal{I}$ is the set of BAs. For that area, the total wind generation is W_i, the total solar generation is S_i and the load is notated L_i. G_i is the conventional dispatchable generation. All W_i, S_i, L_i and G_i are random variables The SGM is calculated as:

$$M_i = G_i - (L_i - (W_i + S_i)),\ \forall\ i \in \mathcal{I} \tag{1}$$

The SGM is, also, a random variable and can be positive or negative, indicating surplus or deficit in the system, respectively, see an example SGM Probability Density Function (PDF) at the upper part of Fig. 1. This means that there is some probability that the SGM realization will be positive and the rest of the probability that it will be negative. All the area under the curve, left of 0, is the cumulative probability that the system will be in a deficit of power, see, again, the upper part of Fig. 1.

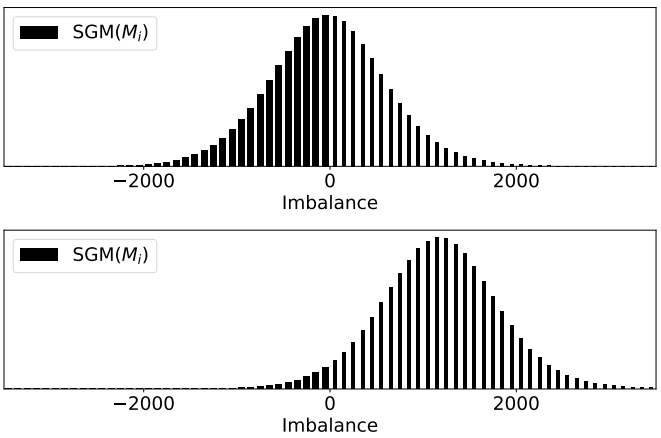

Fig. 1: System power imbalance probability, i.e., SGM, before (upper) and after (lower) the addition of reserve R_i.

The term R_i is the amount of reserve (not a random variable) we need to add to the SGM so that the cumulative probability of deficit is less than an acceptable risk limit set by the TSO. In practice, adding R_i moves the SGM probability curve to the right by R_i MW. This is desirable as we seek to reduce the area left of zero (probability of deficit) to a value less or equal than the risk limit of the TSO. See in the lower part of Fig. 1 the effect of adding reserve R_i to the SGM. Therefore, we can calculate a value for R_i that reduces the probability of power deficit to less or equal than an acceptable risk limit. More formally, there is an R_i such that:

$$P(M_i + R_i \leq 0) \leq RI_i \tag{2}$$

Where RI_i is the acceptable risk taken in BA i by the respective TSO. Every TSO calculates the R_i a-priori and it is given as an input to the method.

C. Problem formulation

The goal is to minimise the total cost of obtaining FRR for the entire Balancing Region (BR) for each time period. Note that, a BR is comprised of many BAs. The objective function and constraints of the proposed formulation are:

$$\mathcal{L} = \min_{\mathbf{r},\hat{\mathbf{r}},\tilde{\mathbf{r}}} \sum_{n\in\mathcal{N}} \pi_n r_n \tag{3a}$$

$$0 \leq r_n \leq \overline{r}_n,\ \forall n \in \mathcal{N} \tag{3b}$$

$$\hat{r}_i = \sum_{n\in\mathcal{N}} B_{i,n} r_n,\ \forall i \in \mathcal{I} \tag{3c}$$

$$\tilde{r}_{i,j} \leq \sum_{b\in\mathcal{B}} |\hat{D}^i_{b,j}| \hat{r}_j,\ \forall\ i,j \in \mathcal{I} \tag{3d}$$

$$\underline{F}_b \leq \sum_{j\in\mathcal{I}} D^i_{b,j} \tilde{r}_{i,j} \leq \overline{F}_b,\ \forall\ i \in \mathcal{I},\ b \in \mathcal{B} \tag{3e}$$

$$R_i \leq \hat{r}_i + \sum_{j\in\mathcal{I}} \tilde{r}_{i,j},\ \forall\ i \in \mathcal{I} \tag{3f}$$

Where, r_n is a decision variable that expresses the sized volume of shared FRR n and $n \in \mathcal{N}$ is the set of available reserves. Note that, each r_n is located in one of the BAs, i. π_n is the associated cost of each FRR. $\overline{r}_n$, is the maximum value of an available reserve n, $\underline{F}_b$ and $\overline{F}_b$ the maximum limit of positive and negative power flow, $\hat{r}_i$ is a variable expressing the total shared reserve sized in BA i and B of size $\mathcal{I}x\mathcal{N}$ is a matrix of $\{0, 1\}$, mapping each r_n to a BA i. In other words, $\hat{r}_i$ is the sum of all r_n located in i. $\tilde{r}_{i,j}$ is a variable expressing the shared reserve between BA j and BA i. D^i is the Power Transfer Distribution Factor (PTDF) calculated considering bus i as reference. $\hat{D}^i$ is similar to PTDF but only the rows that refer to lines adjacent to i are kept and the rest are set to 0.

Constraint (3b) expresses the limits on how much of reserve r_n can be committed. Equation (3c) groups each r_n according to the BA it is located. Constraint (3d) states that the reserve that can be considered as available to flow from BA j to BA i can arrive at its interconnection lines. BA i can use all or some of it. Constraint (3e) enforces, for each BA i, that the $\tilde{r}_{i,j}$ coming from j can go through every line in between, without violating the line capacity limits. Constraint (3f) enforces that for every BA i, the shared reserves that are located inside the area, plus those which can flow from other BA have to be at least equal to the level of reserve R_i.

Constraint (3d) looks similar to the power flow constraints used in DC Optimal Power Flow (OPF). Thinking in terms of power flow applies only to ensure that reserve activation flows from one BA to another are feasible, without violating interconnection capacity limits (i.e. constraint (3c)). In our case, however, constraint (3d), refers to *power availability* and not *power flow*.

Power availability does not have a positive and negative direction. The direction of the reserve power flow is only important when considering its activation. Thus, we do not assign a negative or positive direction on reserve co-sizing. This is because reserves are not *power flows* from one area to the other but rather constitute *power availability*. Reserve volume in one area is not consumed in another area. It is shared (i.e., co-sized), instead in both areas. For example, if BA *A* shares its reserve with BA *B*, this does not mean that this reserve is leaving ($-$ sign) BA *A* to go ($+$ sign) to BA *B*, as power flow would do. Instead, both areas add this reserve to their available reserves (both use a $+$ sign). That is the difference when scheduling reserve availability compared to reserve activation. Thus, when two BAs share reserves, they join some of their uncertainty regarding their SGMs. Subsection II-D provides an overview of the approach followed in [22] and subsection II-E describes the novel approach proposed in this paper to adress this question.

D. Simple sharing of uncertainty

Constraint (3f) assumes that when a BA i needs a certain volume of FRR, no other area will need some of it at the same time. This assumption, of course, is not necessarily accurate. Therefore, extra considerations have to be made to account for the fact that uncertainty coming from all other areas affects area i.

In [22] we developed a simple method in order to address the added uncertainty stemming from the interconnections and

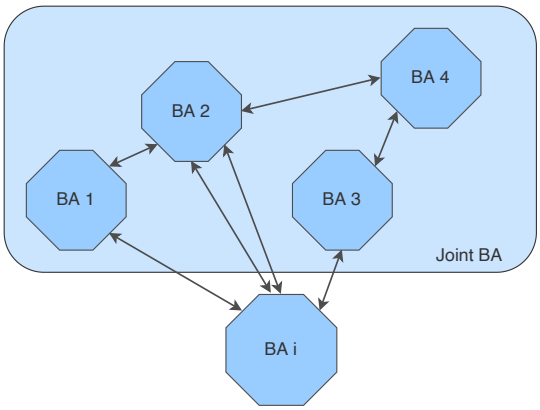

Fig. 2: Illustration of sharing uncertainty principles. The square area is the joint BA that produces the joint SGM, $M_i'(x)$, of equation (4).

we made the following assumptions. A BA i observes the rest of the BR only through the interconnections adjacent to it. Thus, we assume that for i the rest of the region is one united BA without restrictions on power flows within it, see Fig. 2. It follows that, for i, the joint BA beyond its borders has a joint SGM, expressed by the random variable M_i':

$$M_i' = \sum_{j \in \mathcal{I}, j \neq i} M_j \tag{4}$$

However, one can argue that BA i is not exposed to the whole extent of uncertainty stemming from the rest of the region. Instead, it is affected by the total interconnection capacity of BA i, notated as C_i:

$$C_i = \sum_{j \in \mathcal{I}} F_j^{\downarrow,i} \tag{5}$$

C_i is the sum of all interconnection capacities that are adjacent to i:

$$F_j^{\downarrow,i} = |\hat{D}_{b,j}^i \max(\underline{F}_b, \overline{F}_b)|, \forall b \in \mathcal{B} \tag{6}$$

where j is a neighbour of i. The uncertainty to which BA i is exposed is a random variable $\breve{M}_i$:

$$\breve{M}_i(x) = \begin{cases} M_i'(x), & \text{if } x < -C_i \text{ or } x > 0 \\ \int_{x=-\infty}^{-C_i} M_i'(x), & \text{if } x = -C_i \\ \int_{x=0}^{\infty} M_i'(x), & \text{if } x = 0 \end{cases} \tag{7}$$

The yellow curve in Fig. 3 provides a visual representation of eq. (7). BA i is not exposed directly to the joint uncertainty of all its neighbours (notated as M_i') due to the limited capacity of its adjacent interconnections, C_i. Instead, BA i is affected by a reduced section of M_i', which is the one that "passes" through the interconnection C, see the first term in eq. (7). In practice, any part of M_i' that is within the range $[-C_i, 0]$ passes directly to $\breve{M}_i$. What is left of $-C_i$ is perceived by BA i as a power deficit of $-C_i$, therefore, all this probability is accumulated on $-C_i$ (second term of eq. (7)), hence the dotted vertical line in Fig. 3. Similarly for the part of M_i' right of 0 (third term of eq. (7)).

The final SGM of BA i becomes M_i^*:

$$M_i^* = M_i + \breve{M}_i \tag{8}$$

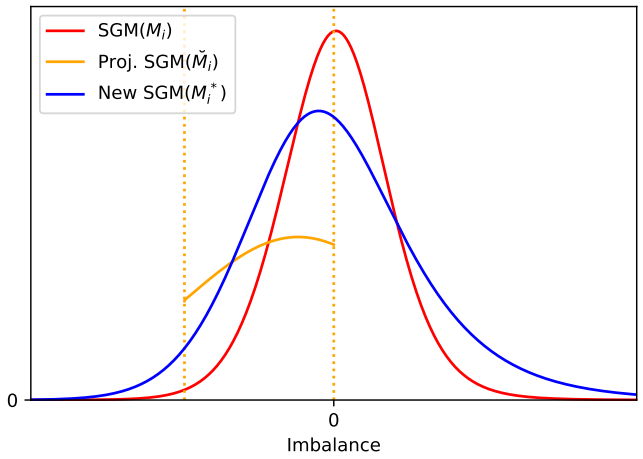

Fig. 3: Qualitative illustration of the SGM update of BA i after consideration of the uncertainty due to interconnections showing the PDF of the initial SGM (M_i) (red line), the PDF of the joint SGM projected through the interconnection ($\breve{M}_i$) (yellow line) and the PDF of the final SGM (M_i^*) (blue line).

Eq. (8) is the addition of random variables M_i and $\breve{M}_i$ via convolution. The new reserve requirement of i, notated as $\hat{R}_i$, is such that:

$$P(M_i^* + \hat{R}_i \leq 0) \leq RI_i \tag{9}$$

The PDFs of M_i, $\breve{M}_i$ and M_i^* are shown qualitatively in Fig. 3. The red curve illustrates the initial SGM of a BA i, M_i, before uncertainty due to interconnections is considered. The yellow curve depicts the uncertainty coming from the joint SGM of neighbour BAs as affected by the interconnection capacity and is notated as $\breve{M}_i$. This curve is described, also, by eq. (7). Finally, the blue curve illustrates the final SGM of BA i, M_i^*. What the yellow curve in the figure and eq. (8) describe is that there is a new source of uncertainty, due to the interconnections, which BA i has to consider. $\breve{M}_i$ is the random variable that describes this uncertainty and can be added to the original SGM of i, M_i, giving the final SGM of i, M_i^*.

$\hat{R}_i$ replaces R_i in the RI_i calculation. What it actually means is that, a-priori, we calculate the SGM for BA i in the worst case condition, when it comes to dependence on interconnections. That is, we include in the reserve capacity sizing of BA i the full interconnection capacity of i, which is the maximum reserve volume that can come from other BAs, regardless if it will be exploited in full by the optimization model (3). Thus, we can be certain, a-priori, that our $\hat{R}_i$ calculation is the most robust when it comes to dependency on the rest of the region for reserves.

A second characteristic of the calculation, that keeps us in the conservative side, is the assumption of one big joint BA beyond BA i (Fig. 2). In practice the different BAs beyond i will not have unlimited interconnections among them, therefore the uncertainty we assume (M_i') is the upper bound of the actual uncertainty that would form by joining the rest of the regions beyond i using finite interconnections.

To facilitate better understanding of the concept of uncertainty sharing, we present an example of the new SGM

calculation $\hat{R}_i$. We create DA probabilistic forecasts based on historical data, as described in subsection II-F. The SGM M_i, is a product of convolution of conventional, wind, solar generation, as well as load distributions. This convolution is implemented using discrete fast Fourier transform (FFT) convolution, see also subsection II-F, therefore any distribution type can be used in their place without extra complexity.

E. Proposed sharing of uncertainty

In the proposed method we retain the assumption that each BA i is exposed to cross-border uncertainty only via the adjacent interconnections. In this case, however, we do not unite the rest of the balancing region into one joint BA, as in Fig. 2. Instead, we consider that, initially, only the neighbouring BAs j contribute to the increased uncertainty of i, separately, via the respective interconnections ($F_j^{\downarrow,i}$).

The steps of the proposed method are described in Fig. 4 The method starts by gathering all the initial SGMs M_i. For each BA i, the following iterative process is followed: We update each BA's SGM by projecting one by one its neighbours via the process described in Fig. 3. Note here that we use M_j^k and $\rightarrow F_j^{\downarrow,i}$, instead of M_i' and C_i in (7). Thus:

$$\breve{M}_j^k(x) = \begin{cases} M_j^k(x), & \text{if } x < -F_j^{\downarrow,i} \text{ or } x > 0 \\ \int_{x=-\infty}^{F_j^{\downarrow,i}} M_j^k(x), & \text{if } x = -F_j^{\downarrow,i} \\ \int_{x=0}^{\infty} M_j^k(x), & \text{if } x = 0 \end{cases} \tag{10}$$

The updated SGM M_i^k is stored as the current SGM and the process is repeated, using the current SGM, until the maximum number of iterations K is reached. When this happens, we use the last current SGMs of the neighbours to update BA i projecting them on its initial SGM. The output of the method is the final SGMs distributions of each country, namely M_i^* which are used in the FRR requirement, $\hat{R}_i$ calculation, similar to (9):

$$P(M_i^* + \hat{R}_i \leq 0) \leq RI_i \tag{11}$$

The method follows an iterative process but it does not converge and we do not expect it do so. At each iteration, the uncertainty from even more remote BAs is propagating towards BA i, which is a desirable property. However, the uncertainty from nodes that are closer is added to the total uncertainty of BA i more than once. Thus, the total uncertainty of BA i will increase in perpetuity. However, we only care that the more distant node's uncertainty, propagating via several paths is taken into account for BA i. This is achieved by repeating the process for as many iterations as the longest path of the graph. In our case study, it is 8 steps as we have a total of 9 countries. Using this approach, we achieve robustness as all contributors to a BA's uncertainty are considered. Thus, the proposed method, similar to [22], is still naive robust, albeit much less naive, as the case studies indicate.

F. Calculating the PMFs

In order to calculate the SGM Probability Mass Functions (PMFs) we first calculate the individual PMFs of conventional,

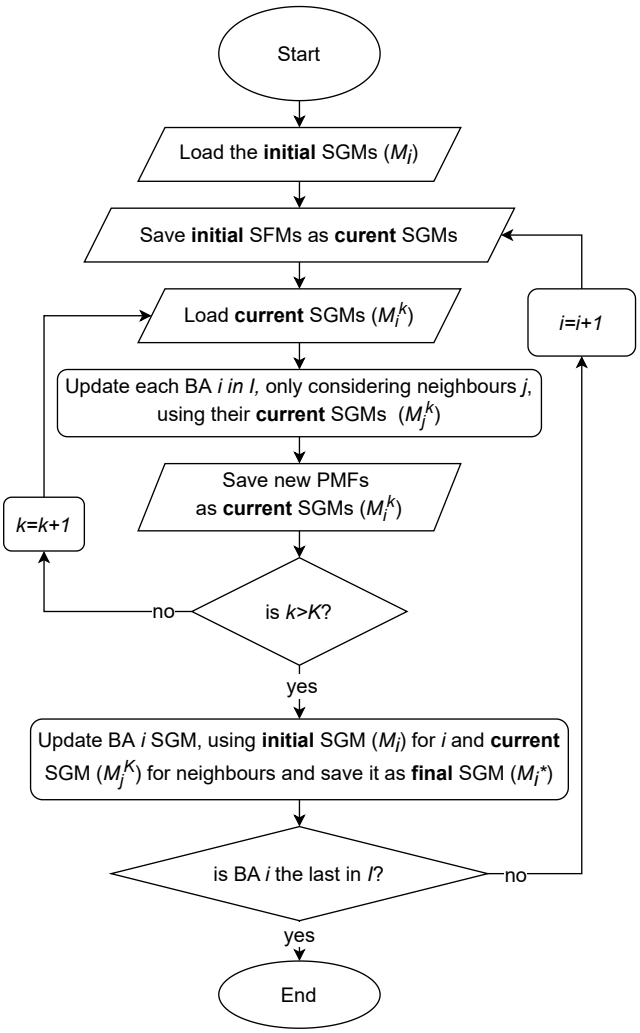

Fig. 4: Flow chart of the proposed method on how to calculate the final SGM of each BA.

wind and solar generation, as well as load, based on historical data from ENTSO-E [24]. Regarding the wind and solar generation, and load, the data consist of timestamps where actual and forecasted values were recorded. For each timestamp the formula of Relative Error (RE) is applied:

$$RE = \frac{A - F}{F} \tag{12}$$

Where, A is the actual value and F the forecasted value. It is worth noting that the denominator in (12) is the forecasted value F since in this concept predictions regarding errors have to be made based on forecasted values.

Consequently, using a fitting algorithm [25] the data are fitted to theoretical PDFs. These PDFs, representing the general behaviour of the relevant random variables, are then scaled [26] by the desirable forecasted values and thus dedicated to the forecasted values PDFs are generated. PDFs are then converted to PMFs with 1 MW bin size so as to be possible to convolve them as 1-D discrete signals.

It is worth noting that, wind and solar generation datapoints with forecasted or actual values close to 0 are susceptible to significant relative errors, degrading the overall quality of the

data sample. In order to alleviate this effect, while maintaining a simplistic approach, and avoiding a possible clustering of the data, datapoints with values up to a certain threshold are excluded from the data set.

The PMF of the conventional generation is analogous to the discrete probability distribution of the possible capacity states, usually known as the Capacity Outage Probability Table (COPT) [27]. In this case though, Forced Outage Rate (FOR) is replaced with the more suitable Equivalent FOR on demand (EFORd) [28]. The conventional generation profile for each country was constructed including information about installed capacity per generation unit and the corresponding EFORd value utilizing data from ENTSO-E [24].

Finally, assuming statistical independence among the individual variables, the PMF of the SGM is equal to the convolution of the previously calculated PMFs. This convolution is performed on sequential steps using FFT and taking into consideration the sign convention of the SGM, see equation (1).

III. Case studies

A. Test case environment and input parameters

The method is developed using the Python programming language [29]. The core algorithm of the method is a mathematical optimization problem. This problem is solved using the Pyomo library of Python [30]. For the solution of the problem, the commercial solver GUROBI is used [31]. For the statistical modelling of the imbalances, we employ standard python libraries such as scipy [32].

The performance of the proposed methodology is tested on a model of the overall power system of the south-east (SE) European region that includes 9 countries, see Fig. 5. The system is reduced in an equivalent where each country is represented by 1 node. The output of the reduction process produces, apart from the graph of the reduced network, the loading of the interconnections, which subsequently determines the remaining interconnection capacity available for FRR sharing. The equivalent reduced model used our case studies is that of [22]. Due to the high level of reduction (several thousand nodes are reduced to 9 nodes), the equivalent model has been created from scratch using the best available approximation for the injection and voltage of the equivalent nodes, as well as the impedance of the equivalent lines. The details behind the reduction methodology are out of scope of this paper.

In order to capture the full range (and extremes) of the Load and RES conditions that system operators may be dealing with and test the efficacy of the proposed methodology in a comprehensive manner, we examine 5 different scenarios, each of which constitutes a different combination of Load and RES levels, as depicted in Fig. 6.

- **Scenario 1**: Low Load - High RES
- **Scenario 2**: High Load - Low RES
- **Scenario 3**: High Load - High RES
- **Scenario 4**: Low Load - Low RES
- **Scenario 5**: Medium Load - Medium RES

As mentioned in subsection II-F, all data for calculating the SGM PMFs, as well as, FRR bids data are taken from historical public data of ENTSO-E [24]. We assume 36 submitted

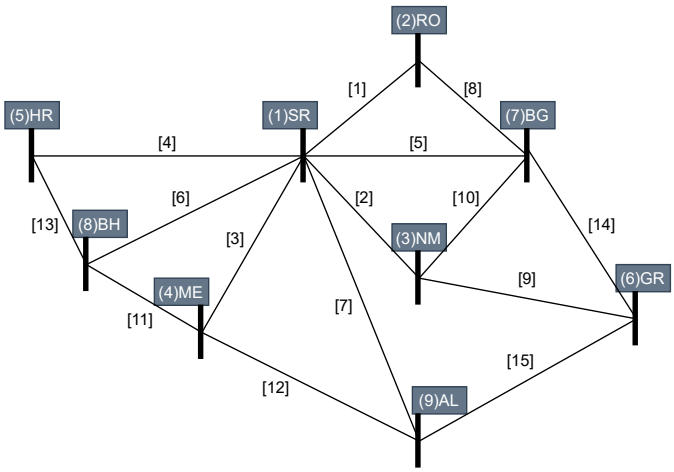

Fig. 5: Illustration of reduced model of South-Eastern European test system.

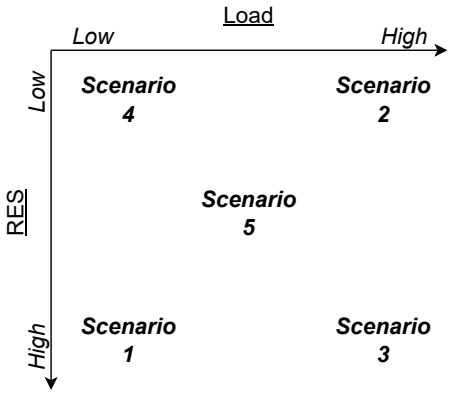

Fig. 6: Combinations of Load and RES levels in each scenario.

FRR bids, 4 in each country in such order: FRR bids SR1-SR4 are in Serbia, RO1-RO4 are in Romania, etc., shown in Table I. The acceptable risk by the TSO's, RI_i is 0.1%. In the illustrations, Scenario 3 is used as an example.

B. Results

1) Baseline: Without cross-border sharing: The simple and proposed methodologies are compared to a baseline case for which no cross-border sharing is allowed. This implies that interconnection capacity limits $\underline{F}_b, \overline{F}_b$ are set equal to zero and R_i is used instead of $\hat{R}_i$ in model (3). In the baseline case, each country can include in its sizing only FRR bids located within its individual system. The committed reserves for the simple case are compared in Fig.s 7 and 8 with the simple and proposed cases, respectively. Even in the baseline case, without cross-border sharing, less expensive results are prioritised. See for example Serbia (FRR bids 1-4) and Montenegro (FRR bids 13-16), where only bids 2 and 14 are used, i.e., the least expensive ones, respectively. The overall committed FRR volume is 16.2GW and the total FRR cost is 23,718 €.

2) Simple cross-border sharing: In this case we use the method of subsection II-D. In model (3), $\hat{R}_i$ is used instead of R_i, and cross-border sharing is allowed. The committed

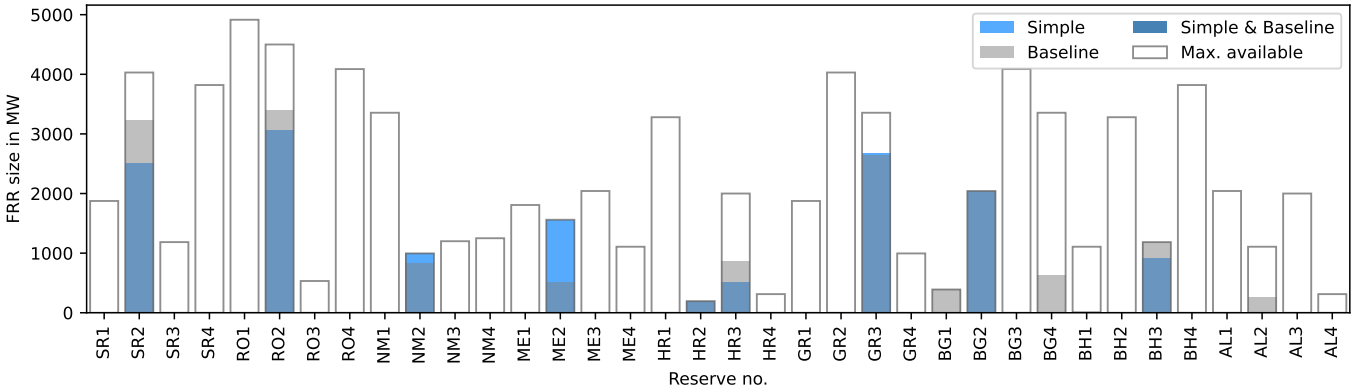

Fig. 7: Committed FRRs under the baseline and the simple method for Scenario 3.

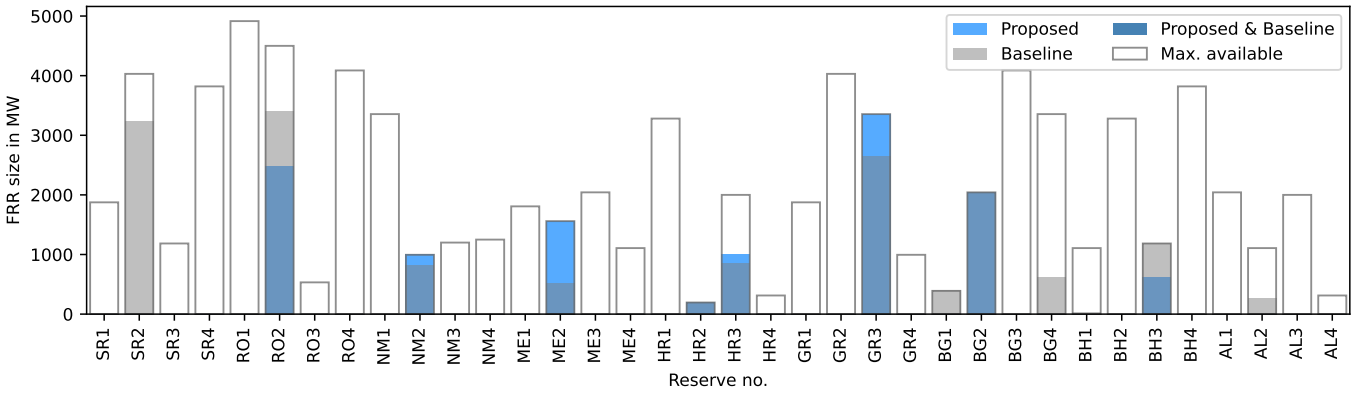

Fig. 8: Committed FRRs under the baseline and the proposed method for Scenario 3.

TABLE I: List of FRR bids submitted in each county including ID, Price and Volume.

ID	Price (€/MW)	Volume (MW)	ID	Price (€/MW)	Volume (MW)
SR1	7	1,875	HR3	4	2,000
SR2	2	4,030	HR4	9	312.5
SR3	23	1,185	GR1	2	1,875
SR4	2.4	3,820	GR2	7	4,030
RO1	7	4,915	GR3	0.4	3,355
RO2	0.9	4,500	GR4	14	995
RO3	31	532.5	BG1	3	390
RO4	6.3	4,087.5	BG2	0.1	2,042.5
NM1	14	3,355	BG3	14	4,087.5
NM2	0.4	995	BG4	6.3	3,355
NM3	15	1,200	BH1	11	1,107.5
NM4	8	1,250	BH2	25	3,280
ME1	4	1,807.5	BH3	2.4	1,185
ME2	0.1	1,560	BH4	23	3,820
ME3	3	2,042.5	AL1	25	2,042.5
ME4	25	1,107.5	AL2	3	1,107.5
HR1	11	3,280	AL3	9	2,000
HR2	0.8	195	AL4	4	312.5

reserves are shown, also, in Fig. 7. Compared to the baseline, one can observe that certain reserves, which are committed in the baseline case, are not included with the proposed method, some others are used less and others more. See, for example, Serbia and Montenegro again. Bid 2 is used less and bid 14 is used more. The total committed FRR volume is 14.4GW and

TABLE II: Reserve requirements for each country under the baseline, simple [22] and proposed methods and the interconnection capacity considered for Scenario 3.

Country	FRR size (MW)			Cumulative Interconnection Capacity (MW)
	Baseline	Simple	Proposed	
SR	3,231	6,347	3,901	6,850
RO	3,403	4,086	3,907	1,377
NM	824	2,477	1,481	3,326
ME	511	1,618	1,289	2,220
HR	1,054	2,085	2,412	2,080
GR	2,646	3,855	3,328	2,464
BG	3,056	4,690	3,726	3,365
BH	1,207	2,582	2,566	2,777
AL	258	1,358	970	2,208

the total FRR cost is 13,961 €. Volume is reduced moderately and costs are reduced significantly, over 40%. This is due to cross-border sharing allowing for less expensive reserves to replace more expensive ones. Indeed, bid 14 in Montenegro is one of the least expensive bids and is fully used in the case of cross-border sharing, contrary to bid 6 which is used less compared to the baseline as it is one of the most expensive ones committed in that case.

3) Proposed cross-border sharing: In this case, we use the proposed method of subsection II-E for updating the SGM in each country. Fig. 8 illustrates the committed reserves

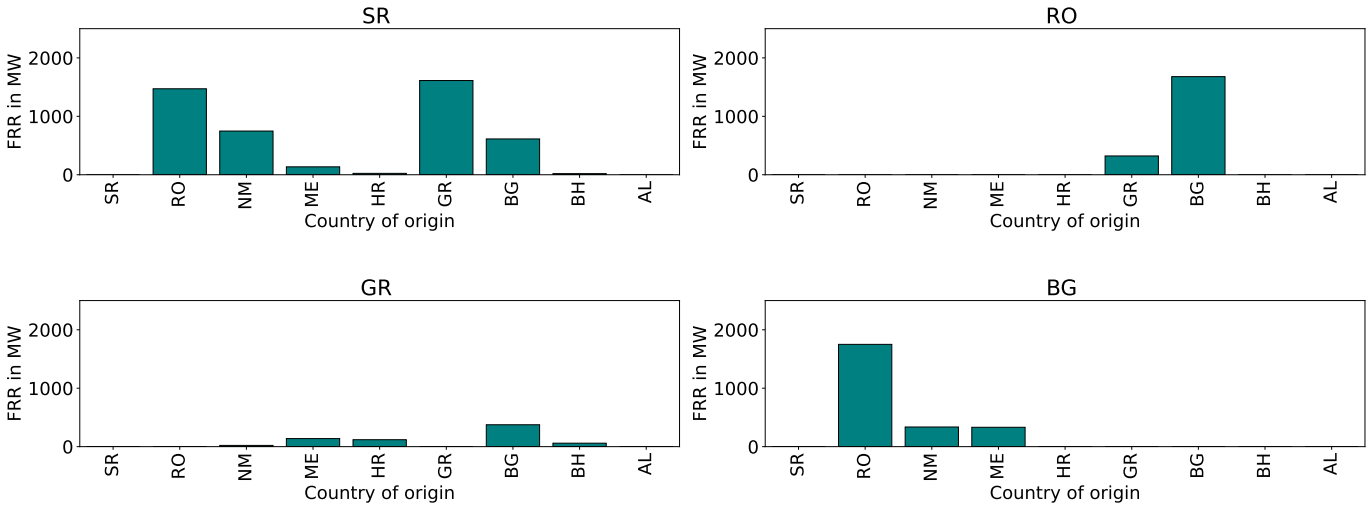

Fig. 9: FRRs considered in the sizing of 4 countries that are located in other countries as calculated by the proposed method for Scenario 3.

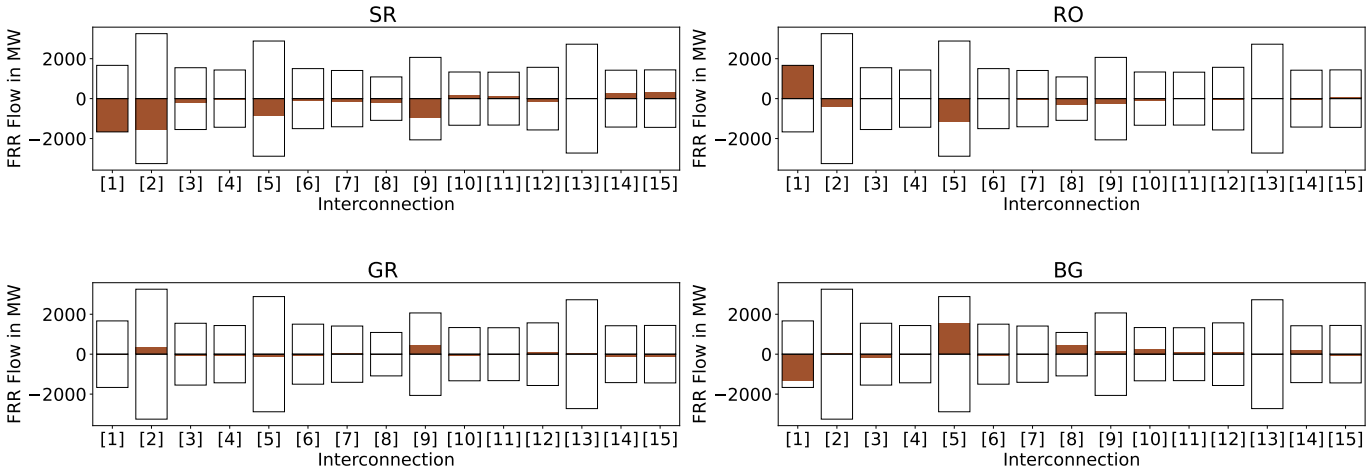

Fig. 10: Interconnection line capacity exploitation at worst case conditions of 4 countries for Scenario 3.

compared to the baseline case. It is clear that FRR volume is reduced significantly. Similar to the simple case, some bids, such as bid 14 in Montenegro are used more, and some, such as bid 2 in Serbia, are used less. However, the decrease in this case is, respectively, larger. The total committed FRR volume for the proposed method case is 9.4 GW and the total FRR cost is 7,354 €. The reduction in volume is 25.1%, whereas in cost, it is 57.2%.

Fig. 9 illustrates how the FRR requirements for 4 countries are covered. Individual countries' a-priori reserve requirements (using R_i) are increasing due to shared uncertainty (see also Table II), however, there is a decrease in the overall FRR sizing volume due to sharing, as the latter effect is more dominant.

Fig. 10 shows the interconnection capacity loading under the individual worst-case condition where all committed reserves are activated for 4 countries. The figures illustrate the enforcement of constraint (3c) which is part of the core optimization problem. We see that limits are respected even when all committed reserves, local and shared, are used from one country.

4) Case comparison: Table III presents the overall FRR volume and costs for the entire region, under the baseline, simple [22] and the proposed method. As discussed in [22], there are two opposing trends when uniting the uncertainty of many countries. One is the increased uncertainty for each individual country due to sharing uncertainty with its neighbours via the interconnections. The opposing trend is that of reserves being shared by more than one country simultaneously (power flow vs. power availability) and less expensive reserves across replacing more expensive ones in the common market that is created. Despite that individual countries have increased reserve requirements, due to increased uncertainty, overall reserve volume is not increased accordingly because, at the same time, one reserve bid can be shared (co-sized) by more than one countries.

The simple method results in similar FRR volumes and an average of 40% reduction in costs, compared to the baseline, see also Table III. Contrary to [22], individual imbalance distributions are calculated with much higher precision in this paper. The more elaborate calculation produced less wide distributions, i.e. with reduced uncertainty which, in turn,

TABLE III: Total FRR volume and costs under the baseline, simple [22] and proposed methods.

	Baseline	Simple method	Change	Proposed method	Change
Scenario [22]					
Volume (MW)	54,743	43,125	-21,2%	31,402	-42,6%
Costs (€)	417,311	288,357	-31,0%	156,317	-62.5%
Scenario 1					
Volume (MW)	9,259	10,037	+8.4%	8,168	-11.7%
Costs (€)	10,170	5,049	-50.3%	5,215	-48.7%
Scenario 2					
Volume (MW)	15,046	14,458	-3.9%	11,639	-22.6%
Costs (€)	22,497	14,109	-37.3%	9,457	-58.0%
Scenario 3					
Volume (MW)	16,190	14,453	-10.7%	12,227	-24.5%
Costs (€)	23,718	13,961	-41.1%	9,939	-58.1%
Scenario 4					
Volume (MW)	7,816	8,645	+10.6%	7,509	-3.9%
Costs (€)	8,723	3,462	-60.3%	4,602	-47.2%
Scenario 5					
Volume (MW)	11,709	11,696	-0.1%	9,392	-19.3%
Costs (€)	14,650	9,379	-36.0%	7,354	-49.8%
Scenarios 1-5					
Volume (MW)	60,020	59,289	-1.2%	48,935	-18.5%
Costs (€)	79,785	45,970	-42.4%	36,567	-54.2%

resulted in more significant increase in uncertainty when the interconnections were considered, i.e. the $M_i + \breve{M}_i$ calculation. As expected, the efficacy of the simple method in reducing FRR volume is not the same as in the [22] case studies. This trend is confirmed by scenarios 1 to 4 in Table III which show that, as uncertainty is increasing progressively from one scenario to the next (here Scenario 1 to 2,4 and finally to Scenario 3) so does the efficacy of the method. However, in all scenarios, cost reduction is still significant.

The new method, proposed in this paper, achieves a significant reduction in both metrics across all scenarios, see Table III. Cost reduction is coming from committing less expensive bids, i.e. the share market drives prices down, and from the overall volume reduction itself. Volume reduction, in turn, comes from the FRR sharing among the countries. We observe a similar correlation between volume and cost savings from the method and how much wider uncertainty a scenario has relatively to others. However, the method produces significant volume and cost reduction for all Scenarios. Moreover, scenarios with high load and generation, such as Scenario 3, are more important as they result in much higher FRR volumes and costs in absolute numbers compared to, for example, Scenario 1.

IV. Conclusion

Cross-border sharing in the sizing stage of FRRs, where interconnection capacities are taken into account is not a well-studied problem. A probabilistic approach to this problem is necessary due to the presence of uncertainty, coming, especially, from non-dispatchable renewable energy sources. A mathematical model that takes into account the special characteristics of reserve power availability, as opposed to power flow during the activation stage, is described in this paper. Moreover, a novel robust approach for calculating increased uncertainty due to interconnections is proposed.

The results have demonstrated that despite the increased uncertainty, due to sharing of reserve capacity among countries, a co-sizing method can yield significant benefits both in terms of sized FRR overall volume, by over 19%, and cost, by over 50% on average using a robust approach. Although interconnection capacities are limiting the extent to which different countries can be jointed in one market, a common market setup that reduces costs is feasible and should be pursued by participating TSOs.

Future work aims at extending the proposed method towards four directions: a) carrying out a sensitivity analysis around the impact of the acceptable risk by the TSOs (which in this work is assumed equal to 0.1%), b) extending the presented analysis to a multi-period framework, considering intertemporal constraints of FRR providers, and c) exploring whether the proposed method can yield higher FRR costs for a subset of the involved countries and devising relevant remuneration mechanisms.

References

[1] P. Pediaditis, C. Ziras, J. Hu, S. You, and N. Hatziargyriou, "Decentralized dlmps with synergetic resource optimization and convergence acceleration," *Electric Power Systems Research*, vol. 187, p. 106467, 2020. [Online]. Available: https://www.sciencedirect.com/science/article/pii/S0378779620302716

[2] P. Pediaditis, D. Papadaskalopoulos, A. Papavasiliou, and N. Hatziargyriou, "Bilevel optimization model for the design of distribution use-of-system tariffs," *IEEE Access*, vol. 9, pp. 132 928–132 939, 2021.

[3] G. Strbac, D. Papadaskalopoulos, N. Chrysanthopoulos, A. Estanqueiro, H. Algarvio, F. Lopes, L. de Vries, G. Morales-España, J. Sijm, R. Hernandez-Serna, J. Kiviluoma, and N. Helisto, "Decarbonization of Electricity Systems in Europe: Market Design Challenges," *IEEE Power and Energy Magazine*, vol. 19, no. 1, pp. 53–63, 2021.

[4] IEA-ENTSAP, "Enhancing the flexibility in TIMES: Introducing Ancillary Services Markets," https://iea-etsap.org/projects/TIMES-BS-Documentation.pdf, 12 2019.

[5] J. Grainger and W. Stevenson, *Power System Analysis*. McGraw-Hill, 1994.

[6] M. G. Webb, "The determination of reserve generating capacity criteria in electricity supply systems," *Applied Economics*, vol. 9, no. 1, pp. 19–31, 1977.

[7] J. Morales, A. Conejo, H. Madsen, P. Pinson, and M. Zugno, *Integrating Renewables in Electricity Markets. International Series in Operations Research & Management Science*. Springer, 2011.

[8] J. M. Morales, A. J. Conejo, and J. Pérez-Ruiz, "Economic valuation of reserves in power systems with high penetration of wind power," *IEEE Transactions on Power Systems*, vol. 24, no. 2, pp. 900–910, 2009.

[9] A. Papavasiliou, S. S. Oren, and R. P. O'Neill, "Reserve requirements for wind power integration: A scenario-based stochastic programming framework," *IEEE Transactions on Power Systems*, vol. 26, no. 4, pp. 2197–2206, 2011.

[10] ENTSO-E, "Network code on load-frequency control and reserves," ENTSO-E, Tech. Rep., 2013.

[11] M. Chazarra, J. I. Perez-Diaz, R. E. Portillo, and A. Hernandez-Bayo, "Manual frequency restoration reserve in spain: Analysis and forecasting," in *2018 15th International Conference on the European Energy Market (EEM)*, 2018, pp. 1–7.

[12] X. Xu, W. Hu, W. Liu, Y. Du, R. Huang, Q. Huang, and Z. Chen, "Look-ahead risk-constrained scheduling for an energy hub integrated with renewable energy," *Applied Energy*, vol. 297, p. 117109, 2021. [Online]. Available: https://www.sciencedirect.com/science/article/pii/S0306261921005535

[13] M. Scherer and G. Andersson, "An outline of an active power reserve sharing process across continental europe," in *2018 IEEE International Energy Conference (ENERGYCON)*, 2018, pp. 1–6.

[14] M. Kayikci, "The european third energy package: How significant for the liberalisation of energy markets in the european union?" *SSRN Electronic Journal*, 01 2011.

[15] P. Pediaditis, K. Sirviö, C. Ziras, K. Kauhaniemi, H. Laaksonen, and N. Hatziargyriou, "Compliance of distribution system reactive flows with transmission system requirements," *Applied Sciences*, vol. 11, no. 16, 2021. [Online]. Available: https://www.mdpi.com/2076-3417/11/16/7719

[16] K. Flinkerbusch and M. Heuterkes, "Cost reduction potentials in the german market for balancing power," *Energy Policy*, vol. 38, no. 8, pp. 4712–4718, 2010. [Online]. Available: https://www.sciencedirect.com/science/article/pii/S0301421510003125

[17] ENTSO-E, "Consultation on the design of the platform for automatic frequency restoration reserve (aFRR) of PICASSO region," ENTSO-E, Tech. Rep., 2017.

[18] A. Fedele, G. D. Benedettto, A. Pascucci, G. Pecoraro, F. Allella, and E. M. Carlini, "European electricity market integration: the exchange of manual frequency restoration reserves among terna and the other TSOs," in *2020 AEIT International Annual Conference (AEIT)*, 2020, pp. 1–5.

[19] P. Zolotarev, M. Gokeller, M. Kuring, , H. Neumann, and E. M. Kurscheid, "Grid control cooperation - a framework for technical and economical cross-border optimization for load- frequency control," in *Cigre 2012 Session*, vol. C2, no. 107, 2012.

[20] F. Baldursson, E. Lazarczyk, M. Ovaere, and S. Proost, "Cross-border exchange and sharing of generation reserve capacity," *The Energy Journal*, vol. 39, 10 2018.

[21] M. A. Matos and R. J. Bessa, "Setting the operating reserve using probabilistic wind power forecasts," *IEEE Transactions on Power Systems*, vol. 26, no. 2, pp. 594–603, 2011.

[22] P. Pediaditis, D. Papadaskalopoulos, N. Hatziargyriou, and D. Prešić, "Cross-border shared sizing of frequency restoration reserves: Insights from the h2020 crossbow project," in *2021 International Conference on Smart Energy Systems and Technologies (SEST)*, 2021, pp. 1–6.

[23] C. Singh, P. Jirutitijaroen, and J. Mitra, *Electric Power Grid Reliability Evaluation: Models and Methods*. Wiley, 12 2018.

[24] "ENTSO-E Transparency Platform," https://transparency.entsoe.eu/.

[25] Scipy, "rv_continuous," https://docs.scipy.org/doc/scipy/reference/generated/scipy.stats.rv_continuous.fit.html, 2022, [Online; accessed 26-July-2022].

[26] N. Mukhopadhyay, *Probability and Statistical Inference*. Marcel Dekker, Inc, 2000.

[27] R. N. Allan and R. Billinton, *Reliability Evaluation of Power Systems*. New York: Plenum, 1984.

[28] AMPS Committee, "IEEE Standard Definitions for Use in Reporting Electric Generating Unit Reliability, Availability, and Productivity," *IEEE Std 762-2006 (Revision of IEEE Std 762-1987)*, pp. 1–75, 2007.

[29] G. van Rossum, "Python tutorial," Centrum voor Wiskunde en Informatica (CWI), Amsterdam, Tech. Rep. CS-R9526, May 1995.

[30] W. E. Hart, C. D. Laird, J.-P. Watson, D. L. Woodruff, G. A. Hackebeil, B. L. Nicholson, and J. D. Siirola, *Pyomo–optimization modeling in python*, 2nd ed. Springer Science & Business Media, 2017, vol. 67.

[31] L. Gurobi Optimization, "Gurobi optimizer reference manual," 2021. [Online]. Available: http://www.gurobi.com

[32] P. Virtanen et al. and SciPy 1.0 Contributors, "SciPy 1.0: Fundamental Algorithms for Scientific Computing in Python," *Nature Methods*, vol. 17, pp. 261–272, 2020.

V. Biography Section

Panagiotis Pediaditis (Student Member, IEEE) received his Diploma in Electrical and Computer Engineering from the National Technical University of Athens (NTUA), Athens, Greece in 2012 and his MSc in Sustainable Energy - Electric Energy Systems from the Technical University of Denmark (DTU), Copenhaghen, Denmark. Since 2018, he is a PhD candidate at NTUA and a researcher for the SmartRUE research group of NTUA. His research interests are smart grids, renewable energy integration, mathematical optimization and machine learning.

Dimitrios Papamatthaiou received his Diploma in Electrical and Computer Engineering from the National Technical University of Athens (NTUA), Greece in 2021. Since 2022, he is working for the Greek TSO, IPTO. His research interests include power system security and renewable energy integration.

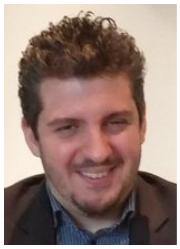

Dimitrios Papadaskalopoulos (Member, IEEE) received the Dipl.-Eng. degree in Electrical and Computer Engineering from the University of Patras, Greece and the Ph.D. degree in Electrical and Electronic Engineering from Imperial College London, U.K., in 2008 and 2013, respectively. He is currently an Assistant Professor in Economic Operation and Analysis of Advanced Electricity Systems at the University of Patras, Greece. His current research focuses on the development and application of decentralized and market-based approaches for the coordination of operation and planning decisions in power systems, employing optimization, game-theoretic and machine learning principles.

Dušan Prešić is currently working as Head of Development department in the Security Coordination Centre SCC Ltd. Belgrade – a regional company devoted to providing Regional Security Coordinator services to the Transmission System Operators. He is SCC's representative in ENTSO-E's Steering Group Regional Coordination. He has a Master's Degree in Electrical Engineering and Computing from the School of Electrical Engineering, University of Belgrade, as well as Bachelor Degree in Electrical Engineering and Computing from the Faculty of Technical Sciences, University of Kragujevac. Mr. Prešić has participated in several Horizon 2020 and Horizon Europe projects as researcher and project manager.

Nikos D. Hatziargyriou (Life Fellow, IEEE) is with the National Technical University of Athens (NTUA), since 1984, Professor in Power Systems, since 1995, and Professor Emeritus, since 2022. He is Part-time Professor at the University of Vaasa, Finland. He has over 10 years of industrial experience as the Chairman and the CEO of the Hellenic Distribution Network Operator (HEDNO) and as the Executive Vice-Chair and Deputy CEO of the Public Power Corporation (PPC), responsible for the Transmission and Distribution Divisions. He has participated in more than 60 R&D projects funded by the EU Commission, electric utilities and industry for fundamental research and practical applications. He has authored or coauthored more than 300 journal publications and 600 conference proceedings papers. He was the Chair and Vice-Chair of ETIP-SNET. He is past EiC of the IEEE Transactions on Power Systems and currently EiC-at-Large for IEEE PES Transactions. He is included in the 2016, 2017 and 2019 Thomson Reuters lists of top 1% most cited researchers. He is the 2020 Globe Energy Prize laureate, recipient of the 2017 IEEE/PES Prabha S. Kundur Power System Dynamics and Control Award and recipient of the 2023 IEEE Herman Halperin Electric Transmission and Distribution Award.